DOI: 10.1002/asia.201500756

Dye-Sensitized Solar Cells

Enhanced Charge Separation Efficiency in Pyridine-Anchored Phthalocyanine-Sensitized Solar Cells by Linker Elongation

Takuro Ikeuchi,[a] Saurabh Agrawal,[a] Masayuki Ezoe,[b] Shogo Mori,*[a] and Mutsumi Kimura*[a]

Abstract: A series of zinc phthalocyanine sensitizers (**PcS22–24**) having a pyridine anchoring group are designed and synthesized to investigate the structural dependence on performance in dye-sensitized solar cells. The pyridine-anchor zinc phthalocyanine sensitizer **PcS23** shows 79% incident-photon to current-conversion efficiency (IPCE) and 6.1% energy conversion efficiency, which are comparable with similar phthalocyanine dyes having a carboxylic acid anchoring group. Based on DFT calculations, the high IPCE is attributed with the mixture of an excited-state molecular orbital of the sensitizer and the orbitals of TiO_2. Between pyridine and carboxylic acid anchor dyes, opposite trends are observed in the linker-length dependence of the IPCE. The red-absorbing **PcS23** is applied for co-sensitization with a carboxyl-anchor organic dye **D131** that has a complementary spectral response. The site-selective adsorption of **PcS23** and **D131** on the TiO_2 surface results in a panchromatic photocurrent response for the whole visible-light region of sun light.

Introduction

Considerable effort has been made to develop various types of sensitizing dyes for dye-sensitized solar cells (DSSCs) using wide-bandgap semiconductors such as titanium oxide (TiO_2).[1,2] Upon light irradiation, the dye adsorbed onto the surface of TiO_2 injects an electron into the conduction band of TiO_2, and the oxidized dye is regenerated to the ground state by electron transfer from redox shuttle in the electrolyte. DSSCs using panchromatic polypyridyl ruthenium complexes have achieved a high power conversion efficiency (PCE) above 11% under one sun conditions.[3] While its absorption range extends close to 900 nm, the low absorption coefficient of the ruthenium complexes is the main drawback to further enhancement of the PCE.[4] Alternatively, π-conjugated macrocycles such as porphyrins and phthalocyanines (Pcs) have attracted a special attention due to their very high extinction coefficients.[5] However, while having two intense absorption bands of the Soret and Q bands in visible light region, porphyrin and phthalocyanine dyes lack absorption in the green spectral region of solar light. Thus, co-sensitization by two dyes with complementary absorption spectra has been examined. Grätzel et al. reported a PCE of over 12% by co-sensitization of D-π-A type porphyrin dye **YD2-*o*-C8** with another organic dye **Y123** in combination with cobalt redox shuttle.[6] We also reported the enhancement of PCE in the co-sensitized DSSCs using sterically protected zinc phthalocyanine dye **PcS15** with an organic dye by the prevention of intermolecular interactions among adsorbed dyes.[7]

Most of sensitizing dyes for DSSCs use carboxylic acid as anchoring groups for the formation of an ester linkage on TiO_2 surface as well as electron accepter units to promote a smooth electron injection. Pyridine,[8] 8-hydroxylquinoline,[9] and 2-(1,1-dicyanomethylene)rhodanine[10] units have been investigated as anchoring groups of sensitizing dyes for DSSCs. These heterocycle ligands can also form coordination bond with TiO_2 surface. Ooyama et al. found highly efficient electron injection through the coordination bond of pyridine anchoring group of D-π-A organic dyes with TiO_2 surface.[8] They also reported that the dyes having the pyridine anchoring group and carboxylic anchoring group tend to be adsorbed on different TiO_2 surface sites. Then, Arakawa et al. exploited the different adsorption behaviors for co-sensitization and found the adsorption of the dye using pyridine anchoring group without decreasing the amount of adsorbed dye using carboxylic acid anchoring group.[11] Thus, the total adsorption density was increased and the photovoltaic performance of the co-sensitized DSSCs was improved, showing employing dyes having two different anchoring groups would be a strategy for co-sensitization.[11] On the other hand, the amount of adsorbed dyes having pyridine anchoring group depends on the structure of the dye framework. Incident-photon to current-conversion efficiency (IPCE) also seems to depend on the length of π-conjugated linker in the sensitizers. However, these points have not been addressed explicitly.

[a] T. Ikeuchi, Dr. S. Agrawal, Prof. Dr. S. Mori, Prof. Dr. M. Kimura
Division of Chemistry and Materials
Faculty of Textile Science and Technology
Shinshu University
Ueda 386-8567 (Japan)
Fax: (+81) 268-21-5499
E-mail: shogmori@shinshu-u.ac.jp
mkimura@shinshu-u.ac.jp

[b] Dr. M. Ezoe
Yamamoto Chemicals Inc.
Yao 581-0034 (Japan)

Supporting information for this article is available on the WWW under http://dx.doi.org/10.1002/asia.201500756.

Results and Discussion

The performance of Pc-sensitized DSSCs has significantly improved by electronic push-pull structure, steric suppression of aggregation, and optimization of adsorption sites.[5c,d] Previously, we reported an overall PCE of 6.4% in DSSCs employing asymmetrical **PcS20** decorated with short alkoxyl chain.[12] In this paper, we examined the applicability of pyridine anchoring group to phthalocyanine dyes. We synthesized novel ZnPc dyes **PcS22**–**24** (Scheme 1) having a pyridine anchoring group

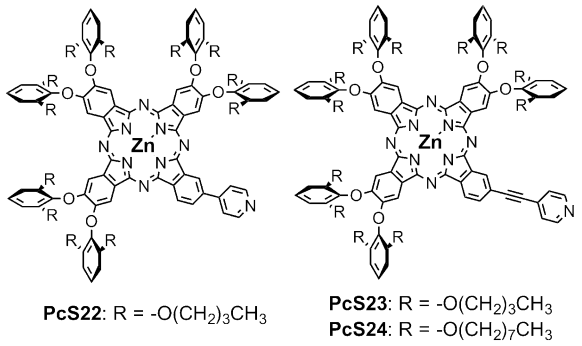

Scheme 1. Molecular structures of **PcS22**–**24** sensitizers.

and different lengths of conjugated linker, and examined their performance in DSSCs. We also applied **PcS23** to the cocktail-type DSSCs by the combination with organic dyes, **D131**, having a carboxylic acid anchoring group.[7,13] DFT calculations for Pcs having carboxylic acid and pyridine anchoring groups on TiO_2 surface were performed to understand charge injection process. The site-selective adsorption of **PcS23** and **D131** on the TiO_2 surface resulted in an increased total dye adsorption density and a panchromatic photocurrent response for the whole visible light region of sun light.

Palladium-catalyzed Stille or Sonogashira coupling reactions with 4-iodophthalonitrile afforded two phthalonitriles having a pyridine ring. The target dyes **PcS22**–**24** were prepared by the statistical condensation of two phthalonitriles in the presence of $Zn(CH_3COO)_2$, and were separated by column chromatography as a second fraction. While the pyridine ring is attached directly to the phthalocyanine macrocycle in **PcS22**, **PcS23** and **PcS24** have an acetylene linker between the phthalocyanine macrocycle and the pyridine anchoring group. Figure 1a shows the absorption spectrum of **PcS23** in toluene, and the spectral data of **PcS22**–**24** are summarized in Table 1. The spectrum of **PcS23** showed a split Q band at 678 and 702 nm, typical of asymmetrical "push-pull" ZnPcs with donor and acceptor

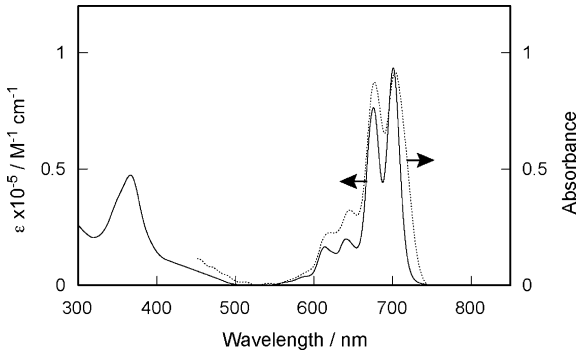

Figure 1. Absorption spectra of **PcS23** in toluene (solid line) and adsorbed on the TiO_2 film (dotted line).

substituents.[14] The width of the split Q band for **PcS23** is almost the same as that of carboxyl-anchor **PcS20** (675 and 695 nm),[13] indicating that the pyridine unit works as a strong electron accepting unit in the asymmetrical ZnPcs. The Q bands of **PcS22** and **PcS23** were slightly red-shifted as compared with the **PcS21** spectrum, which can be attributed to the extension of π-conjugation by the attachment of 4-ethynylpyridine unit with the phthalocyanine macrocycle. The highest occupied molecular orbital (HOMO) and lowest unoccupied molecular orbital (LUMO) energy levels of **PcS22**–**24** were determined from the absorption spectral analyses and the first oxidation potentials of differential pulse voltammetry measurements (Table 1). The HOMO level of **PcS24** having the acetylene linker was lower than that of **PcS23**, also indicating the high electron accepting ability of 4-ethynylpyridine unit.

As the pyridine substituent lie on the same plane of ZnPc macrocycles in **PcS22**–**24**, the coordination between pyridine substituent and central Zn ion leads to the formation of phthalocyanine assemblies.[15] No significant changes in the absorption and fluorescence spectra of **PcS22**–**24** were detected after the addition of a large excess of pyridine. Furthermore, the MALDI-TOF mass spectra of **PcS22**-**PcS24** did not show any molecular ion peaks corresponding to oligomeric phthalocyanine assemblies. These results suggest that the pyridine-anchor **PcS22**–**24** do not form the phthalocyanine assemblies through the formation of intermolecular coordination bonds.

Table 1. Optical and electrochemical data, HOMO and LUMO energy levels, and DSSC device performance parameters of **PcS22**–**24**.

Dye	λ_{max} [nm][a] (log ε [$M^{-1}cm^{-1}$])	E_{ox}[b] [V]	HOMO[c] [V]	LUMO[c] [V]	Adsorption amount[d] $\times 10^{-5}$ [mol cm^{-3}]	Thickness[e] [μm]	V_{oc} [mV]	J_{sc} [mA cm^{-2}]	FF	PCE [%]
PcS22	695 (5.00)	0.24	0.87	−0.90	1.1	12.6+5.0	560	8.1	0.71	3.2
PcS23	702 (4.95)	0.26	0.89	−0.87	3.8	12.6+5.0	580	12.6	0.74	5.4
						4.8+3.4	610	13.5	0.74	6.1
PcS24	702 (4.95)	0.24	0.87	−0.90	0.8	12.6+5.0	600	10.0	0.76	4.6

[a] In toluene. [b] E_{ox} vs. ferrocene/ferrocenium (Fc/Fc^+) were measured by differential pulse voltammetry using dye-stained electrodes in acetonitrile containing 0.1 M Bu_4NPF_6. [c] Vs. normal hydrogen electrode (NHE). [d] Adsorption densities were determined by measuring the absorbance of dyes released from the TiO_2 films by immersing into THF containing acetic acid. [e] Film thicknesses of TiO_2 transparent and scattering layers for DSSCs.

Steric crowding around a ZnPc macrocycle with twelve alkoxy chains at the 2 and 6 positions of peripheral phenoxy units in **PcS22–24** can prevent the pyridine rings of the other dyes from coming close to the central metal.

Porous TiO_2 films on quartz substrate were immersed into toluene solutions of **PcS22–24** to obtain absorption spectra of dye-stained films. The absorption spectrum of **PcS23** adsorbed on a TiO_2 film showed sharp Q bands and the spectrum was in fare agreement with that in toluene solution, revealing the prevention of molecular aggregation among ZnPcs within the adsorbed monolayer of **PcS23** on TiO_2 surface (Figure 1 b). The dye density adsorbed onto the TiO_2 films were determined from the absorbance at the Q band of ZnPc desorbed from the dye-stained TiO_2 film by the treatment with CH_3COOH/THF (Table 1). The adsorption density of **PcS23** was about one-fifth of that of carboxyl-anchor **PcS20** (2.0×10^{-4} mol cm^{-3}),[12] indicating large exposed TiO_2 surface among the sensitizers. The adsorption property of pyridine-anchor organic dyes on TiO_2 surface was investigated by Harima et al.[16] They found a large difference in adsorption equilibrium constant between two dyes possessing pyridine and carboxyl anchors. The low adsorption density of **PcS23** also suggests that the binding of pyridine unit in **PcS23** with TiO_2 surface is weaker than that of carboxyl unit in **PcS20**. Moreover, lacking the acetylene spacer in **PcS22** decreased the adsorption density, which was consistent with the previous report showing lower adsorption density with the dyes having shorter π-conjugation linker.[11] Increasing bulkiness around the ZnPc macrocycle in **PcS24** also diminished the adsorption density.

We fabricated DSSCs using TiO_2 electrodes with electrolytes containing 0.6 M 1,2-dimethyl-3-propylimidazolium iodide (DMPImI), 0.1 M LiI, 0.05 M I_2, 0.5 M *t*-butylpyridine (tBP) in acetonitrile, and the solar cell performances of the **PcS22–24** cells were measured under global AM 1.5 simulated solar conditions (Figure S9). Table 1 lists the short-circuit photocurrent density (J_{sc}), open-circuit voltage (V_{oc}), fill factor (FF), and PCE of **PcS22–24** cells. The PCEs of the **PcS22** and **PcS24** cells were lower than that of the **PcS23** cell, and the PCE value was in the order of **PcS22** < **PcS24** < **PcS23**. This agrees with the order of dye adsorption densities on TiO_2 surface. When the thickness of transparent TiO_2 layer decreased from 13.5 to 4.8 μm, the V_{oc} and J_{sc} values of **PcS23** cell rose from 0.58 to 0.61 V and 12.6 to 13.5 mA cm^{-2} with keeping the same FF values. The **PcS23** cell with a 4.8 μm thickness of transparent TiO_2 layer yields a PCE of 6.1% (Figure 2 a), and the incident-photon to current conversion efficiency (IPCE) at the maximum absorption of the Q band reaches 79% (Figure 2 b). The optimized thickness of TiO_2 film for **PcS23** was 4.8 μm.

To understand the charge transfer nature of photo-excited dye upon adsorption on TiO_2 nanoparticle, we performed DFT calculations for **PcS16-** and **PcS23**-TiO_2 complexes. To reduce the computational cost, alkyl chains of **PcS23** were omitted, which makes the model exactly same as of **PcS24** dye without alkyl chains. Further, **PcS16** (Figure S5) consists of carboxylic acid anchor instead of pyridine anchor as in case of **PcS23/24**.[17] Optimized geometries of **PcS16-** and **PcS23/24**-TiO_2 complexes show (2.03, 2.11) and 2.31 Å bond lengths between

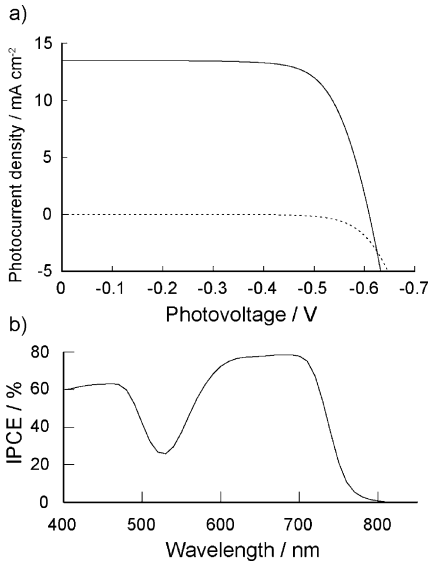

Figure 2. a) Photocurrent voltage curve obtained with DSSC based on **PcS23** under a standard global AM 1.5 solar condition (solid line) and dark current (dotted line). Thickness of TiO_2 transparent layer is 4.8 μm. b) Incident photon-to-current conversion efficiency spectrum for DSSC based on **PcS23**.

dye anchor and attached surface Ti_{5c} atoms respectively (Figure S6). Calculated binding energy between **PcS16** and **PcS23/24** dyes and TiO_2 are −95.04 and −76.13 kJ mol^{-1} respectively. The better binding energy for **PcS16** dye with carboxylate anchor seems reasonable as it forms two covalent bonds with two surface Ti atoms, whereas, pyridine anchors via one coordinate bond with a surface Ti atom. Following optimization, TD-DFT calculations are performed to estimate the optical properties of **PcS23/24**-TiO_2 and **PcS16**-TiO_2 complexes. Computed optical spectrum for **PcS23/24**-TiO_2 shows Q-band peak at 670 nm (1.85 eV) wavelengths (Figure S2). Looking into MOs participated in CT-excitations, we see that HOMO contributes in most of the high intensity photo-excitations and displays localization over phthalocyanine ring (Figure 3), which is characteristically similar to the HOMO of dye (Figure S4). Among unoccupied orbitals, mainly LUMO, LUMO+1 and LUMO+7 participate in CT-excitations. MO plots (Figure 3) as well as MO energy level diagram (Figure S8) suggest that LUMO+1 and LUMO+7 of **PcS23/24**-TiO_2 complex originate from respective reallocation of LUMO and LUMO+1 of **PcS23/24** dye. Considerable localization of LUMO+1 over dye and TiO_2 suggests

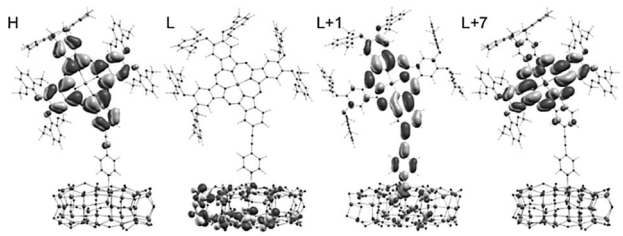

Figure 3. Plotted frontier molecular orbitals HOMO (H), LUMO (L), L+1 and L+7 (isovalue = 0.02 e a.u.$^{-3}$) involved in charge-transfer excitation of the **PcS23/24**–TiO_2 complex.

strong hybridization between dye-TiO_2 orbitals, implying effective charge transfer from photo-excitation dye to TiO_2. Contrary to **PcS23/24**-TiO_2 complex, photo-excited **PcS16**-TiO_2 complex (LUMO + 3, Figure S7) shows only marginal charge localization at dye anchor/TiO_2 interface. This suggests that among the studied systems, mixing of dye/TiO_2 states with pyridine-anchor is stronger than carboxylate-anchor. The coupling of dye/TiO_2 states can be a determining factor of charge injection rate.[18] This seems consistent with the lower J_{sc} and eventually IPCE of **PcS16** sensitized solar cells.

In view of the linker length between the phthalocyanine core and adsorption site, higher IPCE was obtained with the dyes having longer linker (Figure S9). On the other hand, phthalocyanine dyes having carboxylic acid anchoring group, IPCE was decreased with the increase of linker length of the dyes, **PcS15** to **PcS16**.[17] The reason of the opposite trend could be different kinetics of recombination between injected electrons and dye cation. Since pyridine anchor dyes seems to have better molecular orbital hybridization with TiO_2 particle, it would make it easy to not only injection but also recombination with dye cation. Thus, longer linker would be better to reduce the mixing of dye-TiO_2 orbitals to retard charge recombination. On the other hand, for dyes with carboxylic acid anchoring group, shorter linker would be required to have sufficient molecular orbital penetrations for charge injection.

To enhance response of DSSCs using organic dyes in the red-region of solar light, co-sensitization of carboxyl-anchor yellow dye **D131** with **PcS23** was attempted through the site-selective adsorption of two dyes on TiO_2 surface. The surface of TiO_2 electrode was initially covered with **D131** by immersing the TiO_2 electrode into a **D131** solution for 24 hr, followed by immersion into the **PcS23** solution for 24 hr. The adsorption amount of **D131** did not decrease after the treatment with **PcS23**, indicating the successful site-selective adsorption of two dyes on the TiO_2 surface. The DSSC performance of the co-sensitized **D131/PcS23** cell was significantly enhanced in comparison to the **D131** cell. The **D131/PcS23** cell showed almost a double J_{sc} value compared to that of the **D131** cell (Figure 4 a). The IPCE spectra of **D131/PcS23** cell displayed sums of each dyes (Figure 4 b), and the IPCE values corresponding to **D131** in the co-sensitized **D131/PcS23** cell were the same as that of **D131** cell.

Conclusions

In conclusion, we synthesized red-absorbing ZnPc dyes **PcS22–24** with the pyridine anchoring group as sensitizers for DSSCs. The amount of **PcS23** adsorbed on the TiO_2 surface was much lower than that of the carboxyl-anchored ZnPc sensitizer with the same peripheral units. **PcS23** exhibited a PCE of 6.1% when used as a light-harvesting dye on a TiO_2 electrode under one-sun conditions. Based on DFT calculations, the high efficiency seems consistent with a good molecular orbital hybridization between the sensitizer with the pyridine anchoring group and TiO_2 states. In contrast to dyes with carboxylic acid anchoring group, the dyes having longer linker resulted in better charge separation efficiency.

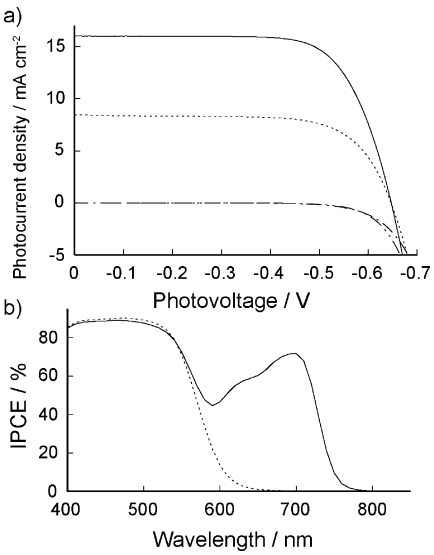

Figure 4. a) Photocurrent voltage curve obtained with DSSCs based on **D131** (dotted line: PCE = 3.8%, J_{sc} = 8.5 mA cm^{-2}, V_{oc} = 650 mV, FF = 0.71, Adsorption amount of **D131** = 22.0 × 10^{-5} mol cm^{-3}) and **D131/PcS23** (solid line: PCE = 7.4%, J_{sc} = 16.0 mA cm^{-2}, V_{oc} = 650 mV, FF = 0.71, Adsorption amounts of **D131** and **PcS23** = 22.0 × 10^{-5} and 2.1 × 10^{-5} mol cm^{-3}) under a standard global AM 1.5 solar condition and dark currents (dashed lines). b) Incident photon-to-current conversion efficiency spectrum for DSSCs based on **D131** (dotted line) and **D131/PcS23** (solid line).

Acknowledgements

This work has been partially supported by Grants-in-Aid for Scientific Research (A) (No. 15H02172) and (B) (No. 22350086) from the Japan Society for the Promotion of Science (JSPS) of Japan.

Keywords: dyes/pigments · energy conversion · phthalocyanines · solar cells · TiO_2

[1] B. O'Regan, M. Grätzel, *Nature* **1991**, *353*, 737.
[2] A. Mishra, M. K. R. Fischer, P. Bäuerle, *Angew. Chem. Int. Ed.* **2009**, *48*, 2474; *Angew. Chem.* **2009**, *121*, 2510 and references therein.
[3] Y. Chiba, A. Islam, Y. Watanabe, R. Komiya, N. Koide, L. Han, *Jpn. J. Appl. Phys.* **2006**, *45*, L638.
[4] M. K. Nazeeruddin, P. Péchy, T. Renouard, S. M. Zakeeruddin, R. Hymphry-Baker, P. Comte, P. Liska, L. Cevey, E. Costa, V. Shklover, L. Spiccia, G. B. Deacon, C. A. Bignozzi, M. Grätzel, *J. Am. Chem. Soc.* **2001**, *123*, 1613.
[5] a) M. Urabani, M. Grätzel, M. K. Nazeeruddin, T. Torres, *Chem. Rev.* **2014**, *114*, 12330; b) K. Ladomenou, T. N. Kitsopoulos, G. D. Sharma, A. G. Coutsolelos, *RSC Adv.* **2014**, *4*, 21379; c) M. E. Ragoussi, M. Ince, T. Torres, *Eur. J. Org. Chem.* **2013**, 6475; d) V. K. Singh, R. K. Kanaparthi, L. Giribabu, *RSC Adv.* **2014**, *4*, 6970.
[6] A. Yella, H. W. Lee, H. N. Tsao, C. Yi, A. K. Chandiran, M. K. Nazeeruddin, E. W. G. Diau, C. Y. Yeh, S. M. Zakeeruddin, M. Grätzel, *Science* **2011**, *334*, 629.
[7] M. Kimura, H. Nomoto, N. Masaki, S. Mori, *Angew. Chem. Int. Ed.* **2012**, *51*, 4371; *Angew. Chem.* **2012**, *124*, 4447.
[8] a) Y. Ooyama, S. Inoue, T. T. Nagano, K. Kushimoto, J. Ohshita, I. Imae, K. Komaguchi, Y. Harima, *Angew. Chem. Int. Ed.* **2011**, *50*, 7429; *Angew. Chem.* **2011**, *123*, 7567; b) Y. Ooyama, T. Nagano, S. Inoue, I. Imae, K. Komaguchi, J. Ohshita, Y. Harima, *Chem. Eur. J.* **2011**, *17*, 14837; c) D. Daph-

nomili, G. Landrou, S. P. Singh, A. Thomas, K. Yesudas, B. K., G. D. Sharma, A. G. Coutsokelos, *RSC Adv.* **2012**, *2*, 12899; d) Y. Ooyama, N. Yamaguchi, I. Imae, K. Komaguchi, J. Ohshita, Y. Harima, *Chem. Commun.* **2013**, *49*, 2548; e) J. Lu, X. Xu, Z. Li, K. Cao, J. Cui, Y. Zhang, Y. Shen, Y. Li, J. Zhu, S. Dai, W. Chen, Y. Cheng, M. Wang, *Chem. Asian J.* **2013**, *8*, 946; f) Y. Ooyama, T. Sato, Y. Harima, J. Ohshita, *J. Mater. Chem. A* **2014**, *2*, 3293; g) C. Stangel, A. Bagaki, P. A. Angaridis, G. Charalambidis, G. D. Sharma, A. G. Coutsolelos, *Inorg. Chem.* **2014**, *53*, 11871.

[9] H. He, A. Gurung, L. Si, *Chem. Commun.* **2012**, *48*, 5910.

[10] J. Mao, N. He, Z. Ning, Q. Zhang, F. Guo, L. Chen, W. Wu, J. Hua, H. Tian, *Angew. Chem. Int. Ed.* **2012**, *51*, 9873; *Angew. Chem.* **2012**, *124*, 10011.

[11] N. Shibayama, H. Ozawa, M. Abe, Y. Ooyama, H. Arakawa, *Chem. Commun.* **2014**, *50*, 6398.

[12] T. Ikeuchi, H. Nomoto, N. Masaki, M. J. Griffith, S. Mori, M. Kimura, *Chem. Commun.* **2014**, *50*, 1941.

[13] a) T. Horiuchi, H. Miura, K. Sumioka, S. Uchida, *J. Am. Chem. Soc.* **2004**, *126*, 12218; b) T. Horiuchi, H. Miura, S. Uchida, *Chem. Commun.* **2003**, 3036; c) R. Y. Ogura, S. Nakane, M. Morooka, M. Orihashi, Y. Suzuki, K. Noda, *Appl. Phys. Lett.* **2009**, *94*, 073308.

[14] J. Mack, N. Kobayashi, *Chem. Rev.* **2011**, *111*, 281.

[15] a) K. Kameyama, M. Morisue, A. Satake, Y. Kobuke, *Angew. Chem. Int. Ed.* **2005**, *44*, 4763; *Angew. Chem.* **2005**, *117*, 4841; b) M. Kimura, T. Hatanaka, Y. Tatewaki, T. Fukawa, H. Shirai, *Chem. Lett.* **2010**, *39*, 946.

[16] Y. Harima, T. Fujita, Y. Kano, I. Imae, K. Komaguchi, Y. Ooyama, J. Ohshita, *J. Phys. Chem. C* **2013**, *117*, 16364.

[17] M. Kimura, H. Nomoto, H. Suzuki, T. Ikeuchi, H. Matsuzaki, T. N. Murakami, A. Furube, N. Masaki, M. J. Griffith, S. Mori, *Chem. Eur. J.* **2013**, *19*, 7496.

[18] a) W. R. Duncan, O. V. Prezhdo, *Annu. Rev. Phys. Chem.* **2007**, *58*, 143; b) S. Agrawal, P. Dev, N. J. English, K. R. Thampi, J. M. D. MacElroy, *J. Mater. Chem.* **2011**, *21*, 11101; c) P. Persson, M. J. Lundqvist, *J. Phys. Chem. B* **2005**, *109*, 11918.

Manuscript received: July 21, 2015
Accepted Article published: July 28, 2015
Final Article published: August 11, 2015